DEVELOPMENT OF 280X29NL ALLOY LIQUEFACTION TECHNOLOGY TO INCREASE THE HARDNESS AND CORROSION RESISTANCE OF CAST PRODUCTS

Turaxodjaev Nodir[1], Saidmakhamadov Nosir[1], Saidkhodjaeva Shokhista[1], Odilov Furkat[1]
[1]Kholmirzaev Nozimjon, Bekchanova Valida,
Tashkent State Technical University, Uzbekistan
Email: anvarovichsarvar908@gmail.com

Abstract - This article, by changing the chemical composition of high-chromium 280X29NL cast iron and processing its composition Ti from 0.93% to 1.78%, the elongation strength of high-chromium cast iron increased and without affecting the hardness of the alloy, Ti addition was added. 'The structure was improved by swelling. The strength of the secondary carbides in the matrix also increased without loss of hardness. In addition, a new brand of alloy 280X29NL (sample 2), which is economically inexpensive and corrosive, was developed without compromising the mechanical properties of the alloy.

Keywords: Alloy, Chrome, Ductile, Microstructure, Carbide, IST - 0,4 Furnace, SNOL - 7,2/1100 Muffle Furnace, "SPEKTROLAB-10M" Equipment, Hardness Measuring Device TK-2M.

1. Introduction

According to the results of research conducted by professors and teachers of the Department of "Casting Technologies" of Tashkent State Technical University on the basis of research conducted at NMP of Navoi Mining and Metallurgical Complex The development of working machine parts from high-chromium cast iron in the form of casting is underway. One of the main problems now is the production of economically inexpensive and high-quality products without compromising the mechanical properties of corrosive high-chromium cast iron. In it is noted that the resistance of the material under conditions of purely abrasive wear depends on the ratio of the hardness of the abrasive (N_a) and the material of the part (N_m) - the coefficient K = N_m: N_a. The critical values of this coefficient have been established: K = 0.6 ÷ 0.7[1,2].

Up to a critical value, when the hardness of the abrasive significantly exceeds the hardness of the metal, the wear resistance of the metal is linearly related to its hardness. If the hardness of the metal becomes close to the hardness of the abrasive, a sharp increase in the wear resistance of the metal occurs.

These results were obtained in tests at small angles of attack (a ≈ 0). In other conditions of wear, these patterns require significant adjustments or do not work.

The resistance of alloys to abrasion is often judged only by their hardness. However, alloys with the same hardness often have different wear resistance (Fig. 1).

The dependences shown in Fig. 1 were obtained by measuring the total hardness of the alloys, which is determined mainly by the hardness of the metal base of the alloy. The presence of carbides with high hardness in the alloy: $(Fe, Cr)_3$ - HV 1080, $(Fe, Cr)_7C_3$ - HV 1240-1550 insignificantly changes the overall hardness of the alloy, but significantly increases its wear resistance, since the hardness of these carbides is equal to or higher than the hardness the most common abrasive is quartz [3, 4].

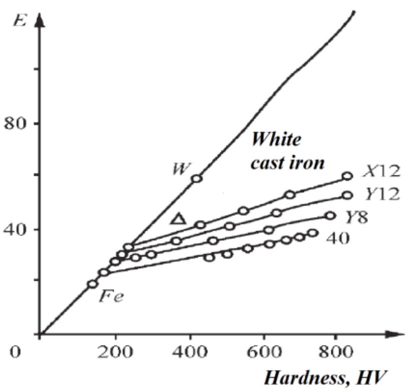

Figure 1: Influence of hardness, composition and structure of alloys on their relative wear resistance (E)

These hard carbides protect the part or specimen from wear (as in this case). To select a material for a part, a machine builder must be guided not only by the hardness of this material, but also by its structure.

High chromium cast iron is mainly used for parts used in operating conditions with high aggressive environment and abrasive wear. Therefore, these cast irons are in great demand by the production and processing industries of the Republic.

High chromium cast irons have high performance properties, from which the production of quality cast parts is important. Because cast iron is alloyed with various alloying elements, including chromium, its alloying properties increase depending on the amount of chromium. In addition, the brittleness of alloy cast irons depends on its microstructure, i.e. in the production of alloyed cast irons it is important to ensure not only the quality of the casting, but also the formation of a microstructure that ensures the corrosion resistance of the cast iron [5, 6].

2. Materials and Methods

At present, the defects in the disks of CEMCO and BARMAK crushers operating on the basis of centrifugal force in the process of crushing ores in the production conditions of NMP of Navoi Mining and Metallurgical Plant and the causes of their formation were analyzed.

Figure 2: A view of a disc cast that has become unusable

Table 1. Chemical composition of the alloy

Brand	Elements, %									
	S	Si	Mn	Cr	Ti	Mo	Cu	Ni	P	S
280X29NL (Sample 2)	2,75	1,87	0,97	14,62	1,72	0,03	0,90	0,16	0,034	0,023

Charcoal composition of the brand 280X29NL		
Cast iron	L2	GOST 4832-95
Cast iron (return)	B 65	GOST 2787-75
Steel	Nickel N12	GOST 1969-2009
Ferrochrome	FX-100	GOST 4757-91
Ferromanganese	FMn-88	GOST 4755-91
Cast iron	FS-45	GOST 1415-93

In order to increase the service life of the part by changing its chemical composition, the results were obtained by providing strength on the surface of the part, which has a high tendency to corrosion under the influence of strong stress and is more likely to crack [7].

The research work of domestic and foreign manufacturers on corrosion-resistant high-chromium cast iron-based cast alloys, as well as research conducted by foreign research institutions and laboratories to extend the service life of cast discs made of high-refractory chromium cast iron.

Figure 3: IST is a high chromium cast iron liquefaction process in a 0.4 induction furnace

High-chromium cast iron was liquefied in sand-clay molds in the IST-0.4 induction furnace in the conditions of NMP enterprise of Navoi Mining and Metallurgical Enterprise and poured into special sand-clay molds.

In order to increase the strength of the discs of crushers operating under high stress from high chromium cast iron, the chemical composition of the shale material for the production of high-chromium cast iron with a strong and dendritic structure was increased on the basis of alloying elements. The results obtained showed that research in this area may yield the expected results.

After coordination, the slag material was heated in an IST-0.4 furnace to a temperature of 1420-1450^0 C, ferroalloys were introduced after the slag was removed, and after holding for 10 minutes, it was poured into a sand-clay mold.

Figure 4: Appearance of disc cast in sand-clay mold

After the casting was cooled in a sand-clay mold, it was heat treated to increase its strength and brittleness.

The sample was cooled in air after being kept in a SNOL-7.2 / 1100 muffle furnace at 980^0 C for 1 hour.

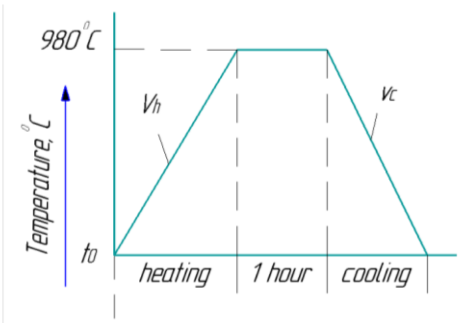

Figure 5: Sample heat treatment graph

SNOL-7.2/1100 muffle furnace was used for heat treatment to improve the internal structure, physical and mechanical properties of cast alloys.

Figure 6: SNOL - 7.2 / 1100 muffle furnace for heat treatment of samples

Figure 7: Air cooling process after heat treatment of samples

SPEKTROLAB-10M equipment, TK-2M hardness tester and METAM RV-23 microscope were used to determine the chemical composition of the samples [8,9,10].

3. Results and Discussions

The chemical composition of the casting material has been developed to increase the ductility of high-chromium cast iron castings in order to increase the service life of CEMCO and BARMAK crushers, which operate mainly under centrifugal force. It was also liquefied in an induction furnace IST-0.4 on the basis of the developed shaft composition and poured into a sand-clay mold. After heat treatment, the sample was examined on the SPEKTROLAB-10M equipment and a uniformly distributed dendritic structure was observed on the surface of the microfields of the samples [11,12].

Figure 8: 100X magnification view using SPEKTROLAB-10M

To determine the hardness of the sample, a hardness measuring device brand TK-2M was used and the hardness was determined to be in the range of 48 HRC - 49 HRC.

In the absence of Ti in the microstructure of high-chromium cast iron, M_7C_3 carbides are formed during eutectic solidification, and phase (a mixture of M_7C_3 and austenite) eutectic austenite dendrites can be seen (Fig. 10). Then, with the addition of Ti, the microstructure of these alloys can contain up to 1.72% Ti, and the phases formed during eutectic solidification can be seen. Figure 10 explores the properties of carbides present in alloys via SEM. In Figure 10 (a), eutectic carbides (M_7C_3) are scattered in the matrix and TiC particles are scattered over the chromium carbides. It can also be seen that titanium carbides are close to eutectic carbides M_7C_3 (Figure 10 (b)).

Figures 11 (a) and 11 (b) show the microstructure of iron by inserting Ti (1.31% Ti) and austenitizing. The samples in Figure 11 (a) were obtained from a microstructure consisting of M_7C_3 carbides, TiC carbides, small amounts of retained austenite, and small secondary carbides embedded in a martensitic matrix at 980⁰C.

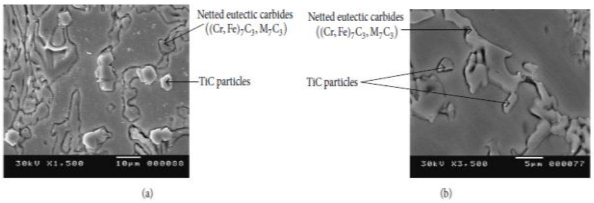

Figure 9: Carbide dispersion properties in the tested high chromium cast irons

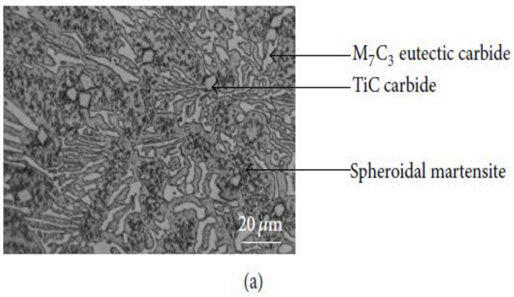

Figure 10: Alloy microstructure components containing 1.78% Ti and (a) processed at 980⁰C

The average diameter of the carbides in the form of these TiC particles is about 3-4 μm, and as most of the TiC increases in the composition of the Ti alloy, the TiC particles are evenly distributed throughout the matrix.

The microstructure of the samples processed at 980⁰C shows small amounts of fine carbides as well as the resulting secondary carbides and spheroid martensite dark on a micrograph (Fig. 12). In this matrix, the secondary carbides are of the same size and uniformly distributed. They are austenite grains after heat treatment, where the mesh eutectic carbides are largely unchanged. Sedimentation of secondary carbides results in a decrease in Cr and C content as austenite. Thus, the C and Cr in austenite also decrease as the dendrites move from high temperature to low temperature. Thus, when cooled from high temperature to room temperature, dendrites are formed. Therefore, during cooling to ambient temperature, austenite turns into dendrite. The amount of austenite in the iron is converted to dendrite during cooling and a small amount of austenite is retained.

Figures 13 (a) -13 (c) show that X-ray diffraction profiles were then compared by casting and heat-treated alloys. The peaks to which the austenite phase and the martensite phase are connected are denoted by γ. Comparisons as a result of heat treatment showed that the dendrites are preserved and significantly increased, while austenite is significantly reduced by the use of heat treatment.

Secondary carbides cannot be observed in the casting state because M_7C_3 eutectic carbides are the most abundant carbides in the gypsum state, followed by the secondary carbides in the very good ($M_{23}C_6$) state.

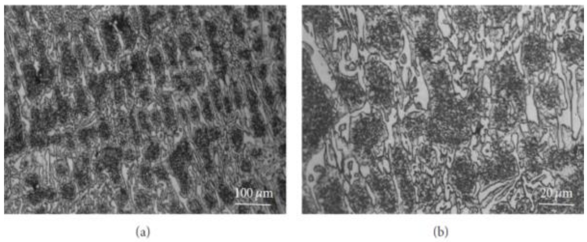

Figure 11: Microstructure of specimens after martensitic and dendritic heat treatment

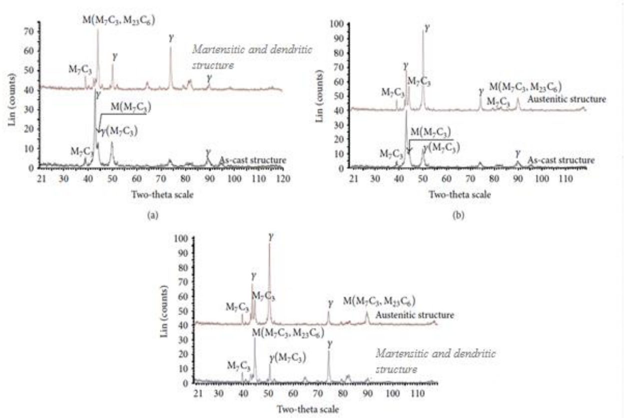

Figure 12: X-ray diffraction profiles of the studied alloys. (a) For martensite and dendrite structure and cast structure. b) the austenitic structure relative to the cast structure. (c) austenitic structure relative to martensitic and dendritic structure

The microstructure of irons machined at 980^0C (Fig. 14) incorporated into the eutectic M_7C_3 martensitic matrix shows the properties of TiC carbides, small amounts of retained austenite, as well as small amounts of secondary carbides. After processing at 980^0 C, a much larger amount of secondary carbides and localized austenite grains were formed faster than other samples processed. Also, as a result of the addition of titanium, the titanium carbides solidified first, and subsequently led to a decrease in the volume fraction of M_7C_3 carbides, which served as the nucleus for proactive austenite dendrites, thereby improving their structure. The addition of barium to white cast iron improves the microstructure [13-21].

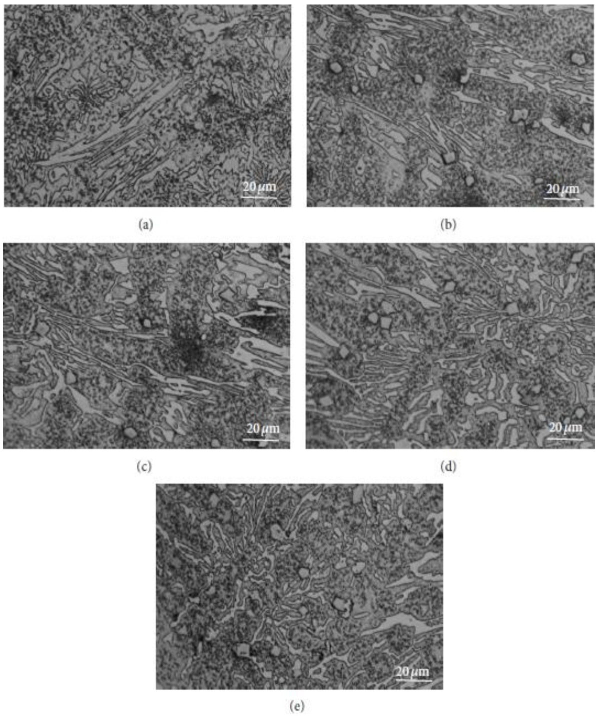

Figure 13: Effect of Ti-addition on microstructure of the heat-treated martensitic irons with (a) 0% Ti, (b) 0.47% Ti, (c) 0.93% Ti, (d) 1.31% Ti, and (e) 1.78% Ti

4. Conclusions

Based on the above data, a technology has been developed to increase the service life of the discs of CEMCO and BARMAK crushers, which operate under the influence of centrifugal force, which is obtained by casting from high-strength chromium cast iron. Based on the analysis of the initial results obtained, the following conclusion was made:

• increased production output resource and developed resource-saving technology in the production of disks;

• the samples were cooled in air after holding for 1 hour at a temperature of 980^0 C in a SNOL-7.2 / 1100 muffle furnace. As a result, a uniformly distributed dendritic structure was observed on the surface of the sample microvilli and the hardness index 48 HRC - 49 HRC was determined using the TK-2M hardness tester to determine the sample hardness;

• when Ti was processed from 0.93% to 1.78%, the tensile strength of high-chromium cast iron was increased and the structure was improved by the addition of Ti without affecting the hardness of the alloy. The strength of the secondary carbides in the matrix also increased without loss of hardness. It is known for high chromium cast irons when Ti is introduced at 1.78%, where the reinforcement of the matrix with secondary carbides resulted in the formation of some areas of TiC agglomeration in the matrix;

• a new brand of alloy 280X29NL (sample 2), which is economically inexpensive and corrosive, was developed by changing the chemical composition of high-chromium 280X29NL cast iron without reducing the mechanical properties of the alloy.

References

[1] Turakhodjaev N. D. et al.; analysis of defects in white cast iron, Theoretical & Applied Science, Volume 6, Pp: 675-682, 2020.

[2] Turakhodjaev N. et al.; Effect of metal crystallation period on product quality, Theoretical & Applied Science. Volume 11, Pp: 23-31, 2020.

[3] Wang Y. et al.; Microstructure and mechanical properties of ultra-lightweight Mg-Li-Al/Al-Li composite produced by accumulative roll bonding at ambient temperature, Materials Science and Engineering, Volume 787, 2020.

[4] Wang Y. et al.; High-strength, ductility and modulus Al–Li/B4C composite with near nanostructure produced by accumulative roll bonding, Journal of Alloys and Compounds. Volume 834, 2020.

[5] Wang Y. et al.; Concurrently improving uniform elongation and strength of ultrafine-grained Al–2Li alloy, Materials Science and Engineering: Volume 792, 2020.

[6] Wang Y. et al. Microstructural evolution, precipitation behavior and mechanical properties of a novel Al–Zn–Mg–Cu–Li–Sc–Zr alloy, Journal of Materials Research, Pp: 1-11, 2021.

[7] Turakhodjaev N. et al.; Analysis of technological solutions for reducing the copper concentration in slags from oxygen-flare smelting of copper sulfide concentrates, Journal of Critical Reviews, Volume 7, Issue 5, Pp: 449-452, 2020.

[8] Bekmirzaev S., Saidmakhamadov N., Ubaydullaev M.; Obtaining sand-clay casting. Theory and practice of modern, Volume 4, Issue 12, P: 112, 2016.

[9] Саидмахамадов Н., Хайдаров У., Эгамбердиев Б. Saidmaxamadov N., Xaydarov U., Egamberdiev B.; Uluchshenie podgotovki texnologiy metodom spesialnogo slivaniya[improvement of technology preparation by special draining method], Ekonomika i sotsium, Volume 4, Pp: 651-660, 2019.

[10] Djahongirovich T. N., Muysinaliyevich S. N.; Important features of casting systems when casting alloy cast irons in sand-clay molds, Academicia: An International Multidisciplinary Research Journal, Volume 10, Issue 5, Pp: 1573-1580, 2020.

[11] Bekmirzaev Sh., Saidmaxamadov N., Ubaydullaev M.; Polucheniya lite v peschano-glinistыe metodom, Teoriya i praktika sovremennoy nauki, Volume 6, Issue 1, Pp: 112-115, 2016.

[12] Saidmaxamadov N. Et al.;. Obshaya texnologiya proizvodstva poroshkovo konstuksionnix materialov[general technology of production of powder construction materials], Ekonomika i sotsium, Volume 4, Pp: 673-680, 2019.

[13] Saidmaxamadov N. Et al.; Texnologiya predotvrasheniya por v otlivax[Pore Prevention Technology in Castings], Ekonomika i sotsium, Volume 4, Pp: 661-672, 2019.

[14] KhaledM. Ibrahim andMervat M. Ibrahim. Heat Treatment in High Chromium White Cast Iron Ti Alloy. Central Metallurgical R&D Institute (CMRDI), P.O. Box 87, Helwan, Cairo, Egypt.

[15] T. Nodir, T. Sherzod, Z. Ruslan, T. Sarvar, & B. Azamat. Studying the scientific and technological bases for the processing of dumping copper and aluminium slags. Journal of Critical Reviews, Volume 7, Issue 11, Pp: 441-444, 2020. doi: http://dx.doi.org/10.31838/jcr.07.05.95.

[16] Nodir, T., Sarvar, T., Andrey, J., & Yahyojon, M.; Mathematical Model for Calculating Heat Exchange. In International Conference on Reliable Systems Engineering, Springer, Cham, Pp: 243-249, 2021.

[17] Umarov, E., Mardonov, U., Abdirakhmonov, K., Eshkulov, A., & Rakhmatov, B. (2021). Effect of magnetic field on the physical and chemical properties of flowing lubricating cooling liquids used in the manufacturing process. IIUM Engineering Journal, Volume 22, Issue 2, Pp: 327-338, 2021. doi: https://doi.org/10.31436/iiumej.v22i2.1768.

[18] Turakhodjaev, N., Tursunbaev, S., Tashbulatov, S., & Kuchkorova, M.; Analysis of technological solutions for reducing the copper concentration in slags from oxygen-flare smelting of copper sulfide concentrates. Journal of Critical Reviews, Volume 7, Issue 5, Pp: 449-452, 2020.

[19] Erkin, U., Umidjon, M., & Umida, S. (2021, September). Application of Magnetic Field on Lubricating Cooling Technological Condition in Metal Cutting Process. In International Conference on Reliable Systems Engineering (pp. 100-106). Springer, Cham.

[20] Turakhodjaev, N., Akramov, M., Turakhujaeva, S., Turakhujaeva, A., Kamalov, J.; Calculation of the heat exchange process for geometric parameters International Journal of Mechatronics and Applied Mechanics, Volume 1, Issue 9, Pp: 90–95, 2021.

[21] E.O. Umarov, U.T. Mardonov, U.K. Shoazimova; Influence of the Magnetic Field on the Viscosity Coefficient of Lubricoolant that is used in the Cutting Process. International Journal of Mechatronics and Applied Mechanics, Volume 8, Issue 2, Pp: 144-149, 2020.